Title	Enhanced spin–orbit torque via interface engineering in Pt/CoFeB/MgO heterostructures
Author(s)	Lee, Hae-Yeon; Kim, Sanghoon; Park, June-Young; Oh, Young-Wan; Park, Seung-Young; Ham, Wooseung; Kotani, Yoshinori; Nakamura, Tetsuya; Suzuki, Motohiro; Ono, Teruo; Lee, Kyung-Jin; Park, Byong-Guk
Citation	APL Materials (2019), 7(3)
Issue Date	2019-03
URL	http://hdl.handle.net/2433/242943
Right	© 2019 Author(s). All article content, except where otherwise noted, is licensed under a Creative Commons Attribution (CC BY) license (http://creativecommons.org/licenses/by/4.0/).
Type	Journal Article
Textversion	publisher

Enhanced spin–orbit torque *via* interface engineering in Pt/CoFeB/MgO heterostructures

Hae-Yeon Lee, Sanghoon Kim (iD), June-Young Park, Young-Wan Oh, Seung-Young Park, Wooseung Ham, Yoshinori Kotani, Tetsuya Nakamura (iD), Motohiro Suzuki, Teruo Ono, Kyung-Jin Lee (iD), and Byong-Guk Park (iD)

ARTICLES YOU MAY BE INTERESTED IN

Enhanced spin–orbit torque *via* interface engineering in Pt/CoFeB/MgO heterostructures

View Online   Export Citation   CrossMark

Hae-Yeon Lee,[1] Sanghoon Kim,[2,3,a] June-Young Park,[1] Young-Wan Oh,[1] Seung-Young Park,[4] Wooseung Ham,[3] Yoshinori Kotani,[5] Tetsuya Nakamura,[5] Motohiro Suzuki,[5] Teruo Ono,[3,6] Kyung-Jin Lee,[7,8] and Byong-Guk Park[1,a]

AFFILIATIONS

[1] Department of Materials Science and Engineering, KAIST, Daejeon 34141, South Korea
[2] Department of Physics, University of Ulsan, Ulsan 44610, South Korea
[3] Institute for Chemical Research, Kyoto University, Uji, Kyoto 611-0011, Japan
[4] Spin Engineering Physics Team, Division of Scientific Instrument, KBSI, Daejeon 34133, South Korea
[5] Japan Synchrotron Radiation Research Institute (JASRI), Sayo, Hyogo 679-5198, Japan
[6] Center for Spintronics Research Network (CSRN), Graduate School of Engineering Science, Osaka University, Osaka 560-8531, Japan
[7] Department of Materials Science and Engineering, Korea University, Seoul 02841, South Korea
[8] KU-KIST Graduate School of Converging Science and Technology, Korea University, Seoul 02841, South Korea

[a] Authors to whom correspondence should be addressed: sanghoon.kim@ulsan.ac.kr and bgpark@kaist.ac.kr.

ABSTRACT

Spin–orbit torque facilitates efficient magnetisation switching via an in-plane current in perpendicularly magnetised heavy-metal/ferromagnet heterostructures. The efficiency of spin–orbit-torque-induced switching is determined by the charge-to-spin conversion arising from either bulk or interfacial spin–orbit interactions or both. Here, we demonstrate that the spin–orbit torque and the resultant switching efficiency in Pt/CoFeB systems are significantly enhanced by an interfacial modification involving Ti insertion between the Pt and CoFeB layers. Spin pumping and X-ray magnetic circular dichroism experiments reveal that this enhancement is due to an additional interface-generated spin current of the non-magnetic interface and/or improved spin transparency achieved by suppressing the proximity-induced moment in the Pt layer. Our results demonstrate that interface engineering affords an effective approach to improve spin–orbit torque and thereby magnetisation switching efficiency.

The electrical manipulation of magnetisation in magnetic nanostructures has opened up new avenues for the further development of spintronic devices because this approach affords simple device miniaturisation and the potential for large-scale integration.[1–3] Conventionally, spin-transfer torque (STT) has been used to control the magnetisation in magnetic multilayer structures,[3,4] particularly for STT-magnetic random access memory (STT-MRAM), in which a spin-polarised current is injected in the direction perpendicular to the film plane. Recently, another type of spin-torque realised by spin–orbit coupling, the so-called spin–orbit torque (SOT),[5,6] has been widely investigated because it allows for efficient

manipulation of the magnetisation using in-plane current, particularly during magnetisation switching[5,6] domain-wall and skyrmion motion.[7–10]

SOT in heavy metal (HM)/ferromagnet (FM)/oxide heterostructures arises from the spin current induced by a charge current via the spin Hall effect (SHE) in the HM and/or the interfacial spin–orbit coupling (ISOC) effect at HM/FM interfaces. This spin current exerts a torque T on the local magnetisation as $T = \tau_{\mathrm{DL}}\hat{m} \times (\hat{y} \times \hat{m}) + \tau_{\mathrm{FL}}\hat{m} \times \hat{y}$,[11,12] where τ_{DL} (τ_{FL}) denotes the damping-like torque (field-like torque), $\hat{m}$ denotes the unit vector along the magnetisation direction, and $\hat{y}$ denotes the unit vector along the

direction perpendicular to both directions of charge current ($\hat{x}$) and inversion symmetry breaking ($\hat{z}$). As τ_{DL} governing SOT-induced magnetisation switching is known to arise mainly due to SHE in HMs,[6,13] most studies have focused on finding HM materials with a large effective spin Hall angle θ_{SH}^{eff} [14–24] for the realisation of energy-efficient SOT-based spintronic devices. On the other hand, it has recently been reported that the HM/FM interface also strongly influences τ_{DL}.[25–33] There are three examples; first, the magnitude and the sign of τ_{DL} are changed by interface modifications,[26,27] which is attributed to the contribution of the ISOC effect to τ_{DL}. Second, θ_{SH}^{eff} of the HM/FM bilayer strongly depends on the spin memory loss[28] or the spin transparency[29] of its interface, thereby indicating that material engineering of HM/FM bilayers can improve the SOT efficiency. Third, the interface itself generates a spin current and thus contributes to the SOT.[31,32] These results suggest that interface engineering could enable further enhancement in the SOT-induced magnetisation switching efficiency.

Among various HM/FM bilayers, a Pt/CoFeB bilayer is a promising candidate for spintronic device application for the following reasons: Pt is a highly conductive HM[33] when compared with other HMs such as β-W[34] or β-Ta,[35] thus reducing Joule heating and thereby power consumption.[33] A CoFeB alloy is a widely used FM in spintronic devices because of its large spin polarisation in conjunction with a crystalline MgO,[36] and a large tunnel magnetoresistance of up to 600% at room temperature has been achieved in CoFeB/MgO-based tunnel junctions.[37] Moreover, Pt/CoFeB/MgO structures have been widely used for voltage-driven spin devices, domain wall, and skyrmion motion devices.[38–41] However, θ_{SH}^{eff} of the CoFeB/Pt bilayer of 0.07[25] is significantly smaller than the highest reported value among Pt/FM bilayers: ~0.2 for Pt/Co samples;[29] thus, it is of interest to further enhance the spin Hall angle in this structure.

In this study, we report significant SOT enhancement in Pt/CoFeB/MgO structures via modification of the Pt/CoFeB interface with the insertion of a thin Ti layer. We observe that the SOT-induced effective fields and magnetisation switching efficiency are doubled upon introducing a 1-nm-thick Ti layer at the Pt/CoFeB interface. The enhancement in SOT or θ_{SH}^{eff} is qualitatively consistent with ferromagnetic resonance (FMR) spin-pumping experiments, in which the inverse SHE voltage of the Pt/CoFeB structure increases by twofold upon Ti insertion. Furthermore, we find that the Ti interfacial layer markedly reduces the magnetic damping constant and the Pt proximity effect. Our results demonstrate the existence of a significant interfacial contribution and suggest that interface engineering can form an efficient approach to improve SOT-induced magnetisation switching.

Samples of Pt(5 nm)/Ti(t_{Ti})/Co$_{32}$Fe$_{48}$B$_{20}$ (CoFeB 1 nm)/MgO(1.6 nm) structures were prepared by magnetron sputtering on thermally oxidised Si substrates with a base pressure of $<4.0 \times 10^{-6}$ Pa $(3.0 \times 10^{-8}$ Torr) at room temperature. The Ti thickness t_{Ti} was varied from 0 nm to 3 nm, and the CoFeB thickness used in this study ranged from 0.9 to 1 nm, which range guarantees strong perpendicular magnetic anisotropy (PMA). Samples were annealed at 150 °C for 40 min under vacuum conditions to induce the PMA. The Hall bar structures with a width of 5 μm were fabricated by photolithography followed by Ar-ion-beam etching. All measurements were carried out at room temperature. For the spin-pumping measurements, the barbell-shaped samples were placed on a coplanar waveguide which generated an alternating magnetic field with a frequency ranging from 8 GHz to 14 GHz. The inverse spin Hall voltage V_{ISHE} was measured as a function of the external magnetic field applied along the sample plane and normal to the barbell shape.[42] The soft x-ray absorption spectroscopy (XAS) at both the Co and Fe L edges was measured using the total electron yield method with the application of 96% circularly polarised incident X-rays under an applied magnetic field of 1.9 T. The X-ray propagation direction was parallel to the film normal and the 10°-tilted magnetic field. The measurements were performed at the BL25SU beam-line at SPring8. Detailed experimental information is available in the literature (including hard XMCD measurements).[43,44] The hard XMCD measurements were performed at the BL39XU beam-line SPring8. A transmission-type diamond X-ray phase retarder with a thickness of 1.4 mm was used to achieve a high degree of circular polarisation (>95%) of X-rays. The X-ray fluorescence yield mode was used to record the X-ray absorption spectra under a magnetic field of 1.9 T. The X-ray propagation direction was parallel to the film normal and the magnetic field. During scanning around the Pt L_3 edge, the helicity of the X-rays was reversed at 0.5 Hz.

We first study the effect of the interfacial modification upon Ti insertion on SOT-induced magnetisation switching using Pt(5 nm)/Ti(t_{Ti})/CoFeB(1 nm)/MgO Hall bar structures, where t_{Ti} is varied from 0 to 3 nm [Fig. 1(a)]. Here, we remark that Ti has a weak spin–orbit coupling[42,45] and that all films considered in this study have perpendicular magnetic anisotropy (PMA). To perform SOT-induced switching experiments, we sweep an in-plane current pulse with a duration of 10 μs while measuring the anomalous Hall resistance R_H between each pulse to detect the magnetisation direction. During the experiment, a magnetic field of 10 mT is applied along the current ($+x$) direction to achieve deterministic switching.[5,46] Figure 1(b) shows the SOT-induced switching results, from which we can infer two points of note. One is the same switching polarity for all samples irrespective of t_{Ti}: under a positive magnetic field, positive (negative) current favours downward (upward) magnetisation. This switching polarity corresponds to the positive θ_{SH}^{eff} of Pt,[5,46] thereby indicating that the Ti insertion layer does not affect the sign of θ_{SH}^{eff}. The second point is that the critical switching current I_C reduces by half when 1 nm of Ti is inserted at the Pt/CoFeB interface. On the other hand, I_C becomes larger for samples with a thicker t_{Ti}, which is attributed to increase in current shunting through the Ti layer with a small θ_{SH}^{eff}. Figure 1(c) depicts the reciprocals of the critical switching current ($1/I_C$) and SOT switching efficiency represented by the critical current density normalised by the anisotropy field $(J_C/B_k)^{-1}$ as a function of t_{Ti}.[47] This confirms that the SOT switching efficiency improves in the regime where t_{Ti} lies between 0.8 and 1.5 nm. We note that the SOT switching efficiency increases by 30% with ~1 nm-Ti insertion, indicating that the reduction in I_c is substantially contributed by the decrease in B_k. Here, we consider that the current is uniformly distributed in the Pt/Ti bilayers since the conductivities of the Pt and the Ti layers are similar to each other, but an order of magnitude larger than that of CoFeB.[22,48] The B_k values are in the supplementary material. There has been a report about effect of Ta insertion between CoFeB and Pt on SOT-driven magnetization switching.[48] However, unlike in our study, these authors did not show an enhancement of the SOT effect with such a heavy-metal insertion layer.
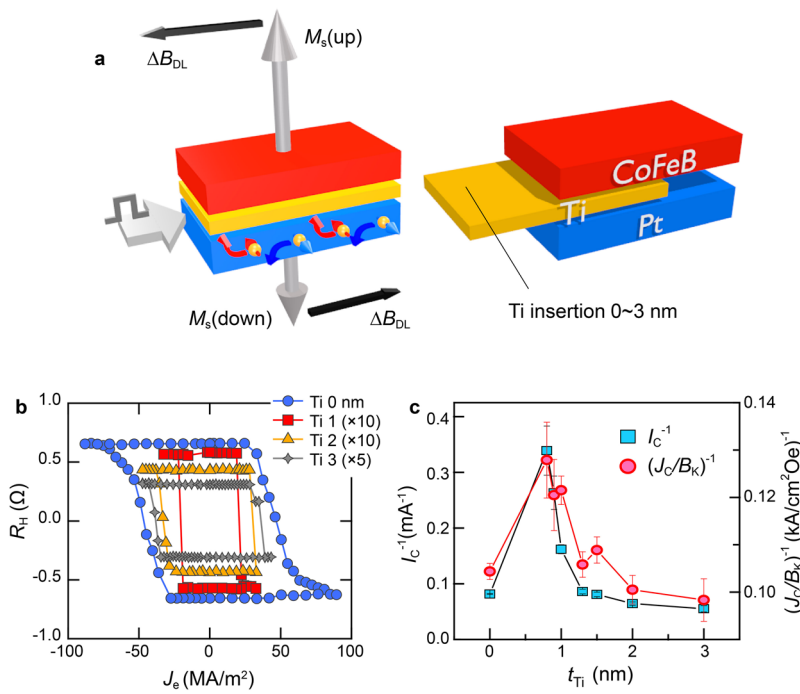
FIG. 1. (a) Schematics of spin–orbit torque (SOT)-driven magnetisation switching (left) and the film structure (right). (b) The current-induced switching curves, anomalous Hall resistance R_H vs. in-plane current density J_e, according to the Ti thickness in Pt/Ti(t_{Ti})/CoFeB/MgO(1.6 nm) structures. The values of R_H are normalised for comparison ($R_{H,Ti(0)}$ = $10R_{H,Ti(1,2)}$ = $5R_{H,Ti(3)}$). (c) The switching efficiency of Pt/Ti(t_{Ti})/CoFeB/MgO (3.2 nm) structures in terms of the reciprocal of I_C (left) and J_C/B_K (right). The error bars represent the standard deviations of the values obtained from three different samples.

In order to quantify the effect of the Ti insertion on the SOT, we measure the SOT-induced effective magnetic fields of Pt/Ti(t_{Ti})/CoFeB/MgO structures using the harmonic lock-in technique.[12,13] As illustrated in Fig. 2(a), the application of an ac current with a frequency of ω generates the first-harmonic Hall voltage ($V^{1\omega}$), which indicates the z-component of magnetisation (M_z), and the second-harmonic Hall voltage ($V^{2\omega}$), which represents the oscillation of magnetisation (ΔM_z) due to SOT-induced effective fields: damping-like (ΔB_{DL}) and field-like (ΔB_{FL}) effective fields. We obtain voltages $V_x^{1\omega,2\omega}$ and $V_y^{1\omega,2\omega}$ when a magnetic field is applied longitudinally ($B = B_x$) and transversely ($B = B_y$) with respect to the current direction, respectively. Figures 2(b) and 2(c) display the $V_x^{2\omega}$ and $V_y^{2\omega}$ values, respectively, for the Pt/Ti(t_{Ti})/CoFeB/MgO samples with t_{Ti} = 1, 2, and 3 nm, while Fig. 2(d) presents $V_x^{2\omega}$ (closed symbols) and $V_y^{2\omega}$ (open symbols) as functions of $B_{x(y)}$ for the Pt/CoFeB/MgO structures without the Ti layer for a current density J_e of 1×10^8 A/cm². The insets depict $V^{1\omega}$, which required to estimate the SOT-induced effective fields (ΔB_{DL} and ΔB_{FL}). ΔB_{DL} and ΔB_{FL} values for all samples are obtained using both the 1st and the 2nd harmonic data with the narrow field regime method (from −100 to 100 mT) which has been suggested by Kim, et al.[11] Here, planar Hall effect and thermal effect were also taken into consideration.[12,46] From this SOT analysis, we found that the magnitudes of both ΔB_{DL} and ΔB_{FL} in the film with t_{Ti} = 1 nm are enhanced by a factor of 2 when compared with those of the film without Ti. This result is consistent with the trend of the switching data presented in Fig. 1.

We estimate θ_{SH}^{eff} using the conventional spin-transfer theory: $\Delta B_{DL}(0)/J_e = (\hbar/2e) \cdot (\theta_{SH}^{eff}/M_s t_{CoFeB})$,[49,6] where $\Delta B_{DL}(0)$ represents the zeroth order of ΔB_{DL},[12] $\hbar$ represents the reduced Planck constant, e represents the elemental charge of an electron, M_s

represents the saturation magnetisation of the CoFeB layers, and J_e represents the current density. The estimated value of the inserted 1-nm-thick Ti film is 0.19 ± 0.03, which is larger than that of the Pt/CoFeB film without Ti (0.13 ± 0.01). This result is consistent with the enhancement in the switching efficiency; however, it is in contrast to previous results,[25,29] wherein θ_{SH}^{eff} is reported to generally decrease upon insertion of an interfacial layer of a 3d metal.

We next examine the origin of the enhancement by performing spin-pumping experiments using ferromagnetic resonance (FMR)[46] for Pt (t_{Pt})/Ti (0, 1 nm)/CoFeB/MgO films, where the Pt thickness t_{Pt} ranges from 2.5 to 16 nm. As schematically illustrated in Fig. 3(a), when the magnetisation is in resonance, a spin current is injected from the CoFeB layer into the Pt layer, which leads to increase in the effective damping constant $\Delta\alpha_{eff}$ in the CoFeB layer along with the generation of a transverse electric voltage via inverse SHE (V_{ISHE}) in the Pt layer. The former is related to the total spin current dissipated in the CoFeB layer, while the latter is due to the spin current injected into the Pt layer. A discrepancy between the two values, $\Delta\alpha_{eff}$ and V_{ISHE}, can be induced if there is generation or extinction of spin current at the interface.[28] The V_{ISHE} value is measured as a function of the external magnetic field, and $\Delta\alpha_{eff}$ is obtained from the variation in the line width of measured V_{ISHE} spectra as a function of the FMR frequency [see Fig. 3(b)]. Figures 3(c) and 3(d) show the Pt thickness dependence of normalized V_{ISHE} by sample resistance and $\Delta\alpha_{eff}$, respectively. When the 1-nm-thick Ti interfacial layer is introduced, V_{ISHE} increases, but $\Delta\alpha_{eff}$ significantly decreases. The doubled magnitude of V_{ISHE} in the Ti-inserted samples demonstrates an increase in θ_{SH}^{eff} of the Pt/Ti/CoFeB structure, which is consistent with the enhanced SOT shown in Figs. 1 and 2. Moreover, the concurrent reduction in $\Delta\alpha_{eff}$ by insertion of 1-nm-thick Ti demonstrates that the increase in the precession angle is an origin
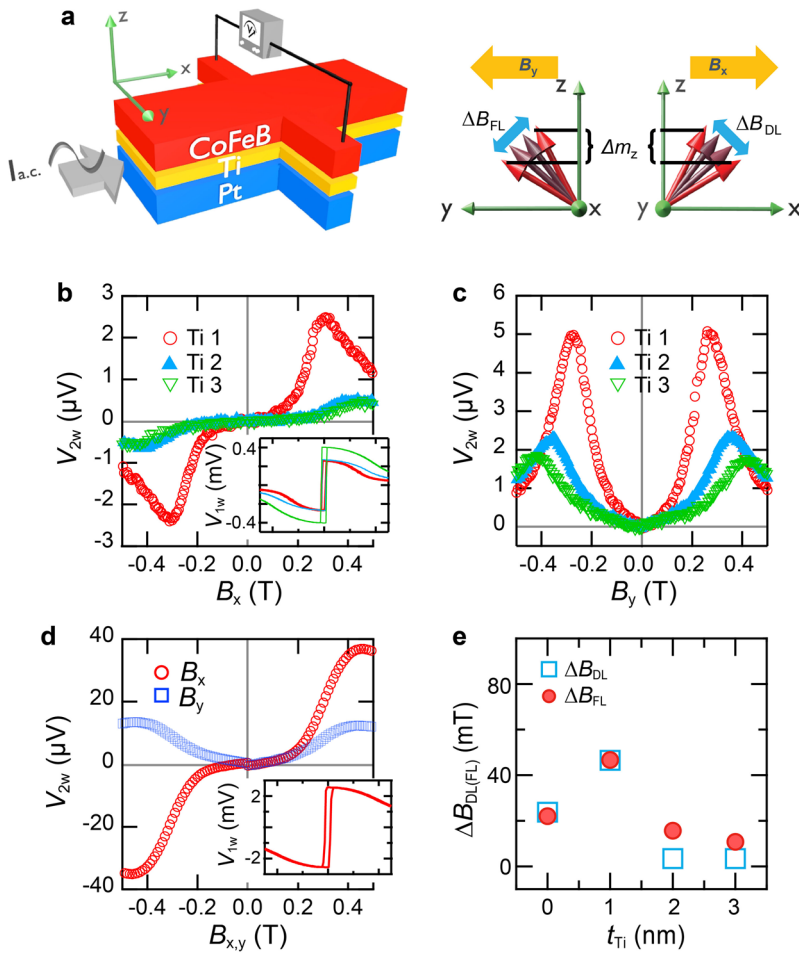
FIG. 2. (a) Schematic of measurement (left) and magnetisation oscillation by ΔB_{DL} and ΔB_{FL} upon applying an ac current (right). Second-harmonic Hall voltages (b) $V_x^{2\omega}$ and (c) $V_y^{2\omega}$ for Pt/Ti(t_{Ti})/CoFeB/MgO samples with different t_{Ti} values. (d) $V_x^{2\omega}$ (solid symbols) and $V_y^{2\omega}$ (open symbols) plots for the Pt/CoFeB/MgO sample. The insets in (b) and (d) depict the first-harmonic Hall voltages $V^{1\omega}$. (e) Damping-like effective field ΔB_{DL} and field-like effective field ΔB_{FL} as functions of t_{Ti}.

of the enhanced V_{ISHE}.[50,51] The decrease in $\Delta\alpha_{eff}$ indicates that the Ti insertion reduces a source of spin current depolarization at the Pt/CoFeB interface that is known to increase the magnetic damping. While the quantitative analysis requires further study, this result suggests that the Ti insertion improves the interfacial spin transparency of the spin current from HM to FM and thus increase θ_{SH}^{eff} or resultant SOT.

We next discuss the possible origins of the enhancement in θ_{SH}^{eff} by the interfacial modification: interface-induced spin current and modified spin transparency of the FM/HM interface. We first consider the modification of the ISOC effect since the Pt/CoFeB interface is replaced by Pt/Ti and Ti/CoFeB interfaces when the Ti layer is introduced. This insertion can enhance the SOT if the ISOC effect of the Pt/CoFeB interface is of opposite sign to the bulk SHE[26] or if the newly generated interface of Pt/Ti provides a positive contribution.[31] Here, we rule out the contribution of the Ti/CoFeB interface because our previous study showed a negligible SOT in the Ti/CoFeB/MgO structure.[27] To verify the modification of the ISOC effect by the Ti layer, we carry out X-ray magnetic circular dichroism (XMCD) measurements at the Fe and Co $L_{2,3}$ edges [Fig. 4(a)]. The orbital-to-spin magnetic moment ratio (m_o/m_s^{eff})

of the Pt/Ti(t_{Ti})/CoFeB/MgO samples, which reflects the magnitude of the ISOC effect of the HM/FM interface,[52,53] is estimated using the sum rule.[54,55] We find that the ratio slightly decreases with increasing t_{Ti}, thus indicating that the ISOC effect cannot be the reason for the enhanced SOT, as shown in Fig. 4(b). Here, we remark that in this respect, the Pt/Ti interface can be a source of spin current and the SOT;[31] however, further studies are required to clarify the spin current generation from the non-magnetic interface. Another possible origin is the improvement of spin current transmission at interfaces which is related to the spin memory loss[28] or spin transparency.[29] As the proximity effect in Pt is a source of spin-current depolarisation, the insertion of the Ti layer may enhance the SOT by suppressing the induced moment in Pt. Thus, we investigate the effect of the Ti interfacial layer on the induced moment in Pt using hard XMCD analysis. Figure 4(c) shows XMCD spectra at the Pt L_3 edges, wherein a clear XMCD signal is observed, thus indicating a finite magnetic moment induced in the Pt 5d orbit for the samples without the Ti layer; however, this signal is completely eliminated by insertion of the 1-nm Ti layer. Thus, the insertion of the Ti layer can enhance the spin transparency and resultant SOT. We observed proximity-induced magnetic moment in the Ti insertion layer, which however is much smaller than that in the Pt
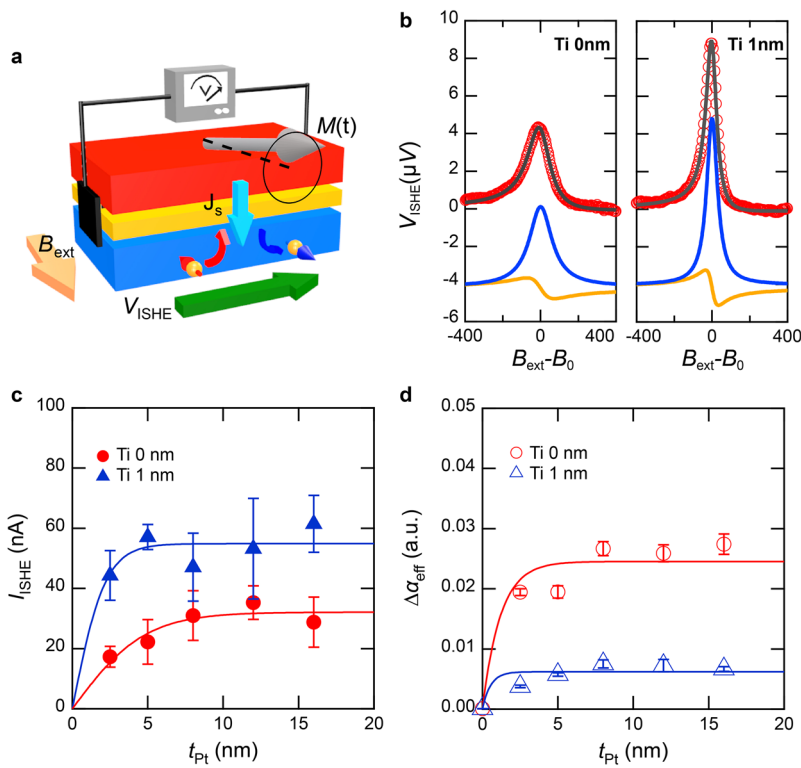
FIG. 3. (a) Schematics of the measurement. (b) Representative V_{ISHE} values in Pt(12 nm)/Ti(0, 1 nm)/CoFeB (2 nm) structures. Symbols indicate measured data, while lines indicate fitting curves. The blue and yellow lines denote the decomposition of symmetric and anti-symmetric components, respectively. (c) V_{ISHE} normalised by sample resistance (I_{ISHE}) vs. Pt thickness t_{Pt} for Pt (t_{Pt})/Ti(0, 1 nm)/CoFeB/MgO samples. (d) The effective damping constant $\Delta\alpha_{eff}$ vs. t_{Pt} for Pt (t_{Pt})/Ti(0, 1 nm)/CoFeB/MgO samples. Parameter t_{Pt} varies from 2.5 to 16 nm. The lines corresponding to V_{ISHE} and $\Delta\alpha_{eff}$ serve as visual guidelines.
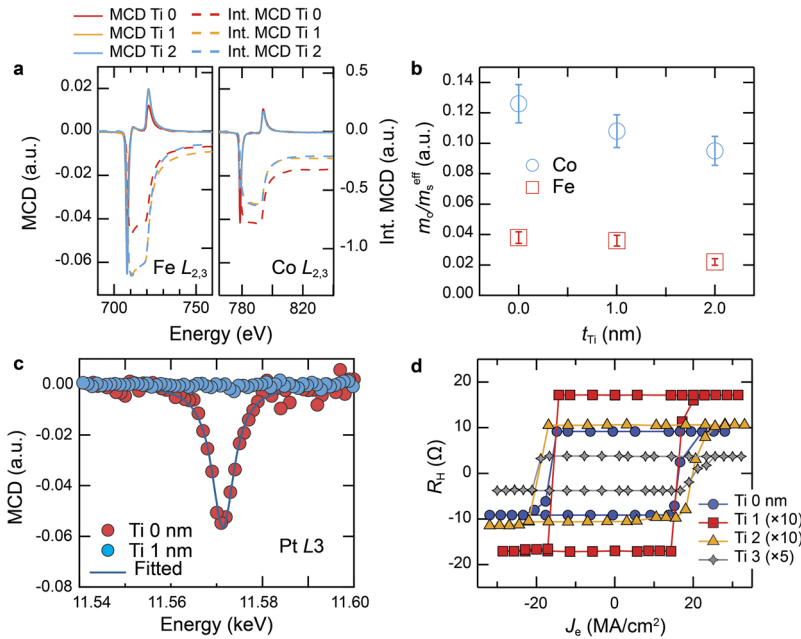

FIG. 4. (a) XMCD and integrated (int.) XMCD spectra at the Fe and Co $L_{2,3}$ edges in the Pt/Ti (0, 1, 2 nm)/CoFeB films. (b) The orbital-to-spin magnetic moment ratio (m_o/m_s^{eff}) values as a function of t_{Ti}. (c) Pt L_3 XMCD spectra of the Pt/Ti (0, 1 nm)/CoFeB/MgO films. (d) Current-induced switching curves as a function of t_{Ti} for Ta/Ti(t_{Ti})/CoFeB/MgO structures, where t_{Ti} = 0–3 nm.

layer.[47] The removal of the proximity-induced moment can also explain the reduction in $\Delta\alpha_{eff}$ upon insertion of the Ti interfacial layer [Fig. 3(d)].[56] This is also supported by results indicating that the SOT monotonously decays in Ta (5 nm)/Ti(t_{Ti})/CoFeB/MgO

structures with increase in Ti interfacial layer thickness, where the proximity effect in Ta is negligible [Fig. 4(d)].

In summary, we demonstrated a large enhancement in the SOT and SOT-induced switching efficiency in a Pt/CoFeB system

by means of interfacial modification involving Ti insertion. The FMR spin-pumping experiments together with XMCD investigations revealed that the enhancement can be attributed to an additional interface-generated spin current and/or improved spin transparency arising due to suppression of the induced moment in the Pt layer. While a quantitative analysis of the effect of the interfacial modification on the SOT requires further experimental and theoretical studies, our experimental results suggest that interface engineering is a promising approach to boost the efficiency of current-induced switching in SOT-based spintronic devices.

See supplementary material for information about the resistivity of each layer, anisotropy field of each film, quantitative SOT analysis, and the proximity effect in the Ti layer.

REFERENCES

[1] I. Žutić, J. Fabian, and S. D. Sarma, Rev. Mod. Phys. **76**, 323 (2004).

[2] A. Brataas, A. D. Kent, and H. Ohno, Nat. Mater. **11**, 372 (2012).

[3] S. S. P. Parkin, M. Hayashi, and L. Thomas, Science **320**, 190 (2008).

[4] D. Apalkov, A. Khvalkovskiy, S. Watts, V. Nikitin, X. Tang, D. Lottis, K. Moon, X. Luo, E. Chen, A. Ong, A. D. Smith, and M. Krounbi, ACM J. Emerging Technol. Comput. Syst. **9**(13), 1 (2013).

[5] I. M. Miron, K. Garello, G. Gaudin, P.-J. Zermatten, M. V. Costache, S. Auffret, S. Bandiera, B. Rodmacq, A. Schuhl, and P. Gambardella, Nature **476**, 189 (2011).

[6] L. Liu, C.-F. Pai, Y. Li, H. W. Tseng, D. C. Ralph, and R. A. Buhrman, Science **336**, 555 (2012).

[7] I. M. Miron, T. Moore, H. Szambolics, L. D. Buda-Prejbeanu, S. Auffret, B. Rodmacq, S. Pizzini, J. Vogel, M. Bonfim, A. Schuhl, and G. Gaudin, Nat. Mater. **10**, 419 (2011).

[8] K.-S. Ryu, L. Thomas, S.-H. Yang, and S. S. P. Parkin, Nat. Nanotechnol. **8**, 527 (2013).

[9] S. Emori, U. Bauer, S.-M. Ahn, E. Martinez, and G. S. Beach, Nat. Mater. **12**, 611 (2013).

[10] W. Jiang, G. Chen, K. Liu, J. Zang, S. G. E. te Velthuis, and A. Hoffmann, Phys. Rep. **704**, 1 (2017).

[11] J. Kim, J. Sinha, M. Hayashi, M. Yamanouchi, S. Fukami, T. Suzuki, S. Mitani, and H. Ohno, Nat. Mater. **12**, 240 (2013).

[12] K. Garello, I. M. Miron, C. O. Avci, F. Freimuth, Y. Mokrousov, S. Blügel, S. Auffret, O. Boulle, G. Gaudin, and P. Gambardella, Nat. Nanotechnol. **8**, 587 (2013).

[13] K. Ando, S. Takahashi, K. Harii, K. Sasage, J. Ieda, S. Maekawa, and E. Saitoh, Phys. Rev. Lett. **101**, 036601 (2008).

[14] A. Hoffmann, IEEE Trans. Magn. **49**, 5172 (2013).

[15] C.-F. Pai, L. Q. Liu, Y. Li, H. W. Tseng, D. C. Ralph, and R. A. Buhrman, Appl. Phys. Lett. **101**, 122404 (2012).

[16] Y. Wang, P. Deorani, X. Qiu, J. H. Kwon, and H. Yang, Appl. Phys. Lett. **105**, 152412 (2014).

[17] H. L. Wang, C. H. Du, Y. Pu, R. Adur, P. C. Hammel, and F. Y. Yang, Phys. Rev. Lett. **112**, 197201 (2014).

[18] B. Gu, I. Sugai, T. Ziman, G. Y. Guo, N. Nagaosa, T. Seki, K. Takanashi, and S. Maekawa, Phys. Rev. Lett. **105**, 216401 (2010).

[19] Y. Niimi, M. Morota, D. H. Wei, C. Deranlot, M. Basletic, A. Hamzic, A. Fert, and Y. Otani, Phys. Rev. Lett. **106**, 126601 (2011).

[20] Y. Niimi, Y. Kawanishi, D. H. Wei, C. Deranlot, H. X. Yang, M. Chshiev, T. Valet, A. Fert, and Y. Otani, Phys. Rev. Lett. **109**, 156602 (2012).

[21] S. Woo, M. Mann, A. J. Tan, L. Caretta, and G. S. D. Beach, Appl. Phys. Lett. **105**, 212404 (2014).

[22] S. Cho, S.-h. C. Baek, K.-D. Lee, Y. Jo, and B.-G. Park, Sci. Rep. **5**, 14668 (2015).

[23] K.-U. Demasius, T. Phung, W. Zhang, B. P. Hughes, S.-H. Yang, A. Kellock, W. Han, A. Pushp, and S. S. P. Parkin, Nat. Commun. **7**, 10644 (2016).

[24] J. W. Lee, Y. W. Oh, S. Y. Park, A. I. Figueroa, G. Van Der Laan, G. Go, K. J. Lee, and B. G. Park, Phys. Rev. B **96**, 064405 (2017).

[25] X. Fan, H. I. Çelik, J. Wu, C. Ni, K. Lee, V. O. Lorenz, and J. Q. Xiao, Nat. Commun. **5**, 3042 (2014).

[26] X. Qiu, K. Narayanapillai, Y. Wu, P. Deorani, D.-H. Yang, W.-S. Noh, J.-H. Park, K.-J. Lee, H.-W. Lee, and H. Yang, Nat. Nanotechnol. **10**, 333 (2015).

[27] Y.-W. Oh, S.-h. C. Baek, Y. M. Kim, H. Y. Lee, K.-D. Lee, C.-G. Yang, E.-S. Park, K.-S. Lee, K.-W. Kim, G. Go, J.-R. Jeong, B.-C. Min, H.-W. Lee, K.-J. Lee, and B.-G. Park, Nat. Nanotechnol. **11**, 878 (2016).

[28] J.-C. Rojas-Sánchez, N. Reyren, P. Laczkowski, W. Savero, J.-P. Attané, C. Deranlot, M. Jamet, J.-M. George, L. Vila, and H. Jaffrès, Phys. Rev. Lett. **112**, 106602 (2014).

[29] W. Zhang, W. Han, X. Jiang, S.-H. Yang, and S. S. P. Parkin, Nat. Phys. **11**, 496 (2015).

[30] W. Zhang, M. B. Jungfleisch, W. Jiang, Y. Liu, J. E. Pearson, S. G. E. te Velthuis, A. Hoffmann, F. Freimuth, and Y. Mokrousov, Phys. Rev. B **91**, 115316 (2015).

[31] V. P. Amin and M. D. Stiles, Phys. Rev. B **94**, 104420 (2016).

[32] S.-h. C. Baek, V. P. Amin, Y.-W. Oh, G. Go, S.-J. Lee, M. D. Stiles, B.-G. Park, and K.-J. Lee, Nat. Mater. **17**, 509 (2018).

[33] M.-H. Nguyen, D. C. Ralph, and R. A. Buhrman, Phys. Rev. Lett. **116**, 126601 (2016).

[34] F. T. N. Vüllers and R. Spolenak, Thin Solid Films **577**, 26 (2015).

[35] A. Jiang, Thin Solid Films **437**, 116 (2003).

[36] Z. Diao, D. Apalkov, M. Pakala, Y. Ding, A. Panchula, and Y. Huai, Appl. Phys. Lett. **87**, 232502 (2005).

[37] S. Ikeda, J. Hayakawa, Y. Ashizawa, Y. M. Lee, K. Miura, H. Hasegawa, M. Tsunoda, F. Matsukura, and H. Ohno, Appl. Phys. Lett. **93**, 082508 (2008).

[38] K.-W. Park, J. Y. Park, S. H. C. Baek, D.-H. Kim, S.-M. Seo, S.-W. Chung, and B.-G. Park, Appl. Phys. Lett. **109**, 012405 (2016).

[39] R. Lo Conte, E. Martinez, A. Hrabec, A. Lamperti, T. Schulz, L. Nasi, L. Lazzarini, R. Mantovan, F. Maccherozzi, S. S. Dhesi, B. Ocker, C. H. Marrows, T. A. Moore, and M. Kläui, Phys. Rev. B **91**, 014433 (2015).

[40] S. Woo, K. Litzius, B. Krüger, M.-Y. Im, L. Caretta, K. Richter, M. Mann, A. Krone, R. M. Reeve, M. Weigand, P. Agrawal, I. Lemesh, M.-A. Mawass, P. Fischer, M. Kläui, and G. S. D. Beach, Nat. Mater. **15**, 501 (2016).

[41] K. Litzius, I. Lemesh, B. Krüger, P. Bassirian, L. Caretta, K. Richter, F. Büttner, K. Sato, O. A. Tretiakov, J. Förster, R. M. Reeve, M. Weigand, I. Bykova, H. Stoll, G. Schütz, G. S. D. Beach, and M. Kläui, Nat. Phys. **13**, 170 (2017).

[42] D.-J. Kim, S.-I. Kim, S.-Y. Park, K.-D. Lee, and B.-G. Park, Curr. Appl. Phys. **14**, 1344 (2014).

[43] T. Nakamura, T. Muro, F. Z. Guo, T. Matsushita, T. Wakita, T. Hirono, Y. Takeuchi, and K. Kobayashi, J. Electron Spectrosc. Relat. Phenom. **144**, 1035 (2005).

[44] M. Suzuki, H. Muraoka, Y. Inaba, H. Miyagawa, N. Kawamura, T. Shimatsu, H. Maruyama, N. Ishimatsu, Y. Isohama, and Y. Sonobe, Phys. Rev. B **72**, 054430 (2005).

[45] C. Du, H. Wang, F. Yang, and P. C. Hammel, Phys. Rev. B **90**, 140407 (2014).

[46] L. Liu, O. Lee, T. Gudmundsen, D. Ralph, and R. Buhrman, Phys. Rev. Lett. **109**, 096602 (2012).

[47] K.-S. Lee, S.-W. Lee, B.-C. Min, and K.-J. Lee, Appl. Phys. Lett. **102**, 112410 (2013).

[48] P. He, X. Qiu, V. L. Zhang, Y. Wu, M. H. Kuok, and H. Yang, Adv. Electron. Mater. **2**, 1600210 (2016).

[49] A. V. Khvalkovskiy, V. Cros, D. Apalkov, V. Nikitin, M. Krounbi, K. A. Zvezdin, A. Anane, J. Grollier, and A. Fert, Phys. Rev. B **87**, 020402(R) (2013).

[50] O. Mosendz, J. E. Pearson, F. Y. Fradin, G. E. W. Bauer, S. D. Bader, and A. Hoffmann, Phys. Rev. Lett. **104**, 046601 (2010).

[51] F. D. Czeschka, L. Dreher, M. S. Brandt, M. Weiler, M. Althammer, I.-M. Imort, G. Reiss, A. Thomas, W. Schoch, W. Limmer, H. Huebl, R. Gross, and S. T. B. Goennenwein, Phys. Rev. Lett. **107**, 046601 (2011).

[52] C. Nistor, T. Balashov, J. J. Kavich, A. Lodi Rizzini, B. Ballesteros, G. Gaudin, S. Auffret, B. Rodmacq, S. S. Dhesi, and P. Gambardella, Phys. Rev. B **84**, 054464 (2011).

[53] M. Kim, S. Kim, J. Ko, and J. Hong, Appl. Phys. Lett. **106**, 102404 (2015).

[54] J. T. Lau, A. Föhlisch, M. Martins, R. Nietubyc, M. Reif, and W. Wurth, New J. Phys. **4**, 98–101 (2002).

[55] C. T. Chen, Y. U. Idzerda, H.-J. Lin, N. V. Smith, G. Meigs, E. Chaban, G. H. Ho, E. Pellegrin, and F. Sette, Phys. Rev. Lett. **75**, 152 (1995).

[56] M. Caminale, A. Ghosh, S. Auffret, U. Ebels, K. Ollefs, F. Wilhelm, A. Rogalev, and W. E. Bailey, Phys. Rev. B **94**, 014414 (2016).